

Violation of the method of images in non-Markovian processes and its connection to stochastic thermodynamics

Takuya Saito,^{1,*} Yuta Sakamoto,^{1,†} and Takahiro Sakaue^{1,‡}

¹*Department of Physical Sciences, Aoyama Gakuin University, Chuo-ku, Sagami-hara 252-5258, Japan*

(Dated: December 2, 2025)

We discuss a failure of the wide-spread method of images solution to describe the time evolution of probability distribution in diffusive processes with memory. For a path that touches a target during stochastic evolution, we define its conjugate twin of reflected path, and show that their path probability ratio obeys a relation analogous to the fluctuation theorem. With a key quantity properly identified as the heat, the resultant thermodynamic interpretation of the processes provides a quantitative basis as well as an intuitive physical picture on how and why the method of images breaks down for non-Markovian processes.

PACS numbers:

Calculation of electric potentials created by a point charge facing conducting planes is a classical subject in electrostatics [1]. A similar situation arises, for instance, in the low Reynolds number hydrodynamics computing fluid flow under stick boundary conditions [3]. Solving such boundary problems is conveniently done thanks to a technique invented by Thomson in 1849 [2], where one places a fictive “image” source so as to satisfy the boundary condition together with the real source. This technique, called the method of images (MI), provides a versatile utility to various boundary problems. One appreciates that its applicability is rooted in the geometry, or more precisely, spatial symmetry of the system under consideration, which manifests in the Laplacian operator in the above examples. As such, the MI works also for the dynamical phenomena, most notably, in the processes described by the diffusion equation, suggesting its use in analyzing the behaviors of random walkers [4, 5]. Indeed, researchers routinely use it in the first passage problems, where one often needs to know the time evolution of probability distribution of relevant stochastic variables under absorbing boundary conditions [4, 5]. Given its power and handiness, however, it is also important to figure out the limitations [6–13]. Rather obviously, the MI cannot be used in systems with potential $U(x)$ that breaks the spatial symmetry. Even without potential, however, it also breaks down in systems with memory, i.e., the non-Markovian processes, but this fact seems not to be well appreciated at present. Although recent works have demonstrated that the use of MI in non-Markovian process leads to erroneous results [11–13], its underlying physics has not been clarified yet.

Here, we analyze the structure of path probability of non-Markovian random walkers in the context of the first passage problem. For a specific first passage path, we construct its conjugate twin of spatially reflected path

and demonstrate that their path probability ratio creates an analogous family member of the fluctuation theorem conventionally based on temporal reverse [14–20]. This allows us to quantify the violation of the MI in non-Markovian processes in terms of heat [21], the statistical property of which is amenable to the stochastic thermodynamics analysis. As a demonstration, we employ the fractional Brownian motion (fBm) [11, 13, 23–25] as a paradigm of non-Markovian walkers to reveal its thermodynamic aspect.

Method of image in diffusion process revisited— Consider one-dimensional random walk in unbounded domain. Let $P_0(x, t|x_0)$ be the probability distribution function (PDF) of the position of random walkers with initial location $x = x_0$. For Markovian walkers, it is given by the solution of diffusion equation $\partial_t P(x, t|x_0) = \partial_x^2 P(x, t|x_0)$ with initial condition $P(x, 0|x_0) = \delta(x - x_0)$ and natural boundary condition, i.e., vanishing probability at infinity [26–29]. In a first passage problem, one considers a diffusive process starting from $x_0 > 0$ under an absorbing boundary at $x = 0$, and asks the time evolution of PDF $P(x, t|x_0)$ in the physical domain $x \geq 0$. The MI provides the solution $P(x, t|x_0) = P_0(x, t|x_0) - P_0(x, t|-x_0)$, where the second term is the contribution from an image “anti-walker” starting at $x = -x_0$ [4]. Why does it work here? The standard reasoning is that it solves the diffusion equation and satisfies both initial and boundary conditions.

Path probability analysis - A deeper insight can be obtained by looking at paths of individual random walkers. Up to time $t(> 0)$, some walkers remain in the positive domain, but others touch the boundary and absorbed. Since we are interested in the PDF of the survival walkers, it takes the form

$$P(x, t|x_0) = P_0(x, t|x_0) - P_D(x, t|x_0), \quad (1)$$

where $P_D(x, t|x_0)$ is the PDF of the absorbed, hence, dead walkers to be subtracted from $P_0(x, t|x_0)$ to satisfy the condition imposed by the absorbing boundary. Although Eq. (1) is generic and holds in the entire domain, one may often focus only on the positive domain

*Electric mail: tsaito@phys.aoyama.ac.jp

†Electric mail: sakamoto2021@phys.aoyama.ac.jp

‡Electric mail: sakaue@phys.aoyama.ac.jp

$x \geq 0$, which constitutes a physical domain in the context of first passage problem. One then finds the correspondence $P_D(x, t|x_0) = P_0(x, t|x_0)$ in the MI solution, which, however, turns out to be valid only for memoryless, i.e., Markovian walkers (Fig. 1).

To see the impact of memory, we consider a Gaussian non-Markovian process. Here and in what follows, for simplicity, we discretize time such that $t = N\Delta t$ with a time increment Δt , and use the step number N and the time t interchangeably, while a continuum form is immediately found in an appropriate limit. Let $|\Delta x\rangle = (\Delta x_1, \Delta x_2, \dots, \Delta x_N)^\top \in \mathbb{R}^N$ be a N -step process with stationary increment, and let a symmetric matrix $D = (D_{ij}) \in \mathbb{R}^{N \times N}$ denote its covariance $D_{ij} = \langle \Delta x_i \Delta x_j \rangle$. Defining a path $\{x_i\}_0^N = (x_0, x_1, \dots, x_N)$ with $x_i = x_0 + \sum_{k=1}^i \Delta x_k$, its path probability [30, 31] given an initial position $x_0 (> 0)$ is

$$P[\{x_i\}_0^N] \sim \exp[-I(|\Delta x\rangle)], \quad (2)$$

where $I(|\Delta x\rangle) = \langle \Delta x | \Gamma | \Delta x \rangle / 2$ with $\Gamma = D^{-1}$. Let $\{x_i\}_{0,n}^N$ be a path of dead walkers, hereafter called “dead path”; it arrives, at least once, at the boundary with $n (\leq N)$ being the first arrival time. We then split the path into two parts; $\{x_i\}_{0,n}^N := (\{x_i\}_0^n, \{x_i\}_n^N)$, and alongside decompose the displacement vector as $|\Delta x\rangle := (|\Delta y\rangle, |\Delta z\rangle)$, where $|\Delta y\rangle = (\Delta x_1, \Delta x_2, \dots, \Delta x_n)^\top \in \mathbb{R}^n$

and $|\Delta z\rangle = (\Delta x_{n+1}, \Delta x_{n+2}, \dots, \Delta x_N)^\top \in \mathbb{R}^m$ represent the initial n steps up to the first arrival and the remaining $m (= N - n)$ steps, respectively. We also introduce the corresponding block decomposition of the matrices D, Γ ;

$$D = \begin{pmatrix} D^I & B \\ B^\top & D^{II} \end{pmatrix}, \quad \Gamma = \begin{pmatrix} \Gamma^I & \Omega \\ \Omega^\top & \Gamma^{II} \end{pmatrix}, \quad (3)$$

where $D^I \in \mathbb{R}^{n \times n}$, $D^{II} \in \mathbb{R}^{m \times m}$, $B \in \mathbb{R}^{n \times m}$ and $B^\top \in \mathbb{R}^{m \times n}$ is the transpose of B . The same decomposition applies to Γ . The action is now written as $I(|\Delta x\rangle) = I_I(|\Delta y\rangle) + I_{II}(|\Delta z\rangle) + \Lambda(|\Delta y\rangle, |\Delta z\rangle)$ with

$$\begin{aligned} I_I(|\Delta y\rangle) &= \frac{1}{2} \langle \Delta y | \Gamma^I | \Delta y \rangle \\ I_{II}(|\Delta z\rangle) &= \frac{1}{2} \langle \Delta z | \Gamma^{II} | \Delta z \rangle \\ \Lambda(|\Delta y\rangle, |\Delta z\rangle) &= \langle \Delta z | \Omega^\top | \Delta y \rangle \end{aligned} \quad (4)$$

To discuss a connection with the MI, we define a path $\{\bar{x}_i\}_{0,n}^N := (\{-x_i\}_0^n, \{x_i\}_n^N)$, hereafter called “reflected path”, which is obtained from the original dead path by spatially reflecting the first passage path, see Fig. 1 (d). Since only Λ in Eq.(4) is odd under the reflection while other terms are even, one finds the probability ratio between the original and its reflected paths

$$\frac{P[\{x_i\}_{0,n}^N]}{P[\{\bar{x}_i\}_{0,n}^N]} = \exp[-2\Lambda[\{x_i\}_{0,n}^N]]. \quad (5)$$

For Markovian processes, D and Γ are diagonal matrices, hence, all the off-diagonal block matrices are null. Since Eq. (5) then states that the original and reflected paths are equally probable, summing over all the pertinent paths, we obtain $P_D(x, N|x_0) = P_{\bar{D}}(x, N|\bar{x}_0)$, where $P_{\bar{D}}(x, N|\bar{x}_0)$ is the PDF of the reflected dead walkers. In such reflected paths, the walker starts at $x = \bar{x}_0 (= -x_0)$ and crosses the boundary at $x = 0$ to reach the final position $x (> 0)$ after N steps. Since such paths with $\bar{x}_0 < 0$ and $x > 0$ necessarily cross the boundary, these paths are unrestricted, hence

$$P_{\bar{D}}(x, N|\bar{x}_0) = P_0(x, N| -x_0), \quad (x_0 > 0, x > 0) \quad (6)$$

where we recall that P_0 is defined for unrestricted walk under natural boundary condition. Combining the above two equalities, the MI construction $P_D(x, N|x_0) = P_0(x, N| -x_0)$ follows, see Fig. 1 (a).

Thermodynamic interpretation - The above discussion highlights the quantity Λ as a measure of the non-Markovianity, which generally invalidates the use of the MI. An apparent similarity of Eq. (5) to the local detailed balance, a key relation in fluctuation theorem [14–20] may evoke an interpretation of Λ as heat. A caveat is that the conventional fluctuation theorem combines the temporal reverse path with the original, which falls into Σ -stochastic entropic functional according to the classification [20], whereas a pair of the MI paths with the

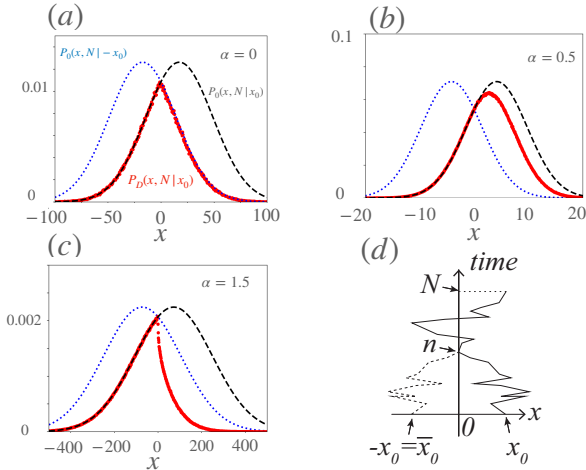


FIG. 1: (a)-(c) Plots of PDFs $P_D(x, N|x_0)$ (red) and $P_0(x, N|x_0)$ (black dashed) in Eq. (1) after $N = 10^3$ steps starting from $x_0 = 300^{\alpha/2}$ for (a) Markovian walker and (b) anti-persistent or (c) persistent non-Markovian walker. Also shown in each panel is $P_0(x, N| -x_0)$ (blue dotted). As a model of non-Markovian walker, we adopt the fBm with anomalous exponent $\alpha (\neq 1)$ for mean square displacement. $P_0(x, N|\pm x_0)$ is the Gaussian function with the mean $\pm x_0$ and the variance $2(N\Delta t)^\alpha$, while $P_D(x, N|x_0)$ is obtained by numerical simulation (see SI). (d) Schematic spatiotemporal plots of the original and the reflected paths with solid and dashed lines, respectively, for the time period $[0, N]$ along vertical time-axis. The reflected path is constructed by folding $\{x_i\}_{0,n}^N$.

spatial reflection creates a notable subclass in the Λ -stochastic entropic functionals. We show below that the quantity $\Lambda[\{x_i\}_{0,n}^N]$ appearing in Eq. (5) is related to the heat.

Let us fix a specific first passage path $\{x_i\}_0^n$ and inquire its consequence on the subsequent dynamics. To this end, we rewrite the action as

$$I(|\Delta x\rangle) = I_{\text{eff}}(|\Delta y\rangle, |\Delta z\rangle) + I_1^{(0)}(|\Delta y\rangle), \quad (7)$$

where

$$I_{\text{eff}}(|\Delta y\rangle, |\Delta z\rangle) = \frac{1}{2} \langle \Delta z - (\Gamma^{\text{II}})^{-1} f | \Gamma^{\text{II}} | \Delta z - (\Gamma^{\text{II}})^{-1} f \rangle \quad (8)$$

and $I_1^{(0)}(|\Delta y\rangle) = \langle \Delta y | (D^{\text{I}})^{-1} | \Delta y \rangle / 2$. This form results from completing square with respect to $|\Delta z\rangle$, where the transformation introduces a “force” $|f(|\Delta y\rangle)\rangle := -\Omega^{\text{T}} |\Delta y\rangle \in \mathbb{R}^m$, which depends on the specific first passage path. Examples of such a force is shown in Fig. 2 for cases of sub-diffusive and super-diffusive fBms. The conditional path probability given the first passage path $\{x_i\}_0^n$ is then identified as

$$P[\{x_i\}_n^N | \{x_i\}_0^n] \sim \exp[-I_{\text{eff}}(|\Delta y\rangle, |\Delta z\rangle)]. \quad (9)$$

The quadratic form of the path probability, see Eq (8), indicates the relation $|\Delta z\rangle = (\Gamma^{\text{II}})^{-1} |f\rangle + |\eta\rangle$, where $|\eta\rangle \in \mathbb{R}^m$ is the noise vectors with $\langle \eta_i \rangle = 0$ and $\langle \eta_i \eta_j \rangle = (\Gamma^{\text{II}})^{-1}_{ij}$. Its m -th component, $\Delta z_m = \sum_{j=1}^m (\Gamma^{\text{II}})^{-1}_{mj} f_j + \eta_m$ describes the time evolution from x_{N-1} to x_N under a given history $\{x_i\}_0^{N-1}$, which is analogous to the algorithm of Hosking method widely used to generate non-Markovian trajectories in numerical simulations [22, 23]. Operating Γ^{II} from the left to the preceding vector equation, we obtain $\Gamma^{\text{II}} |\Delta z\rangle = |f\rangle + |\xi\rangle$ with $|\xi\rangle = \Gamma^{\text{II}} |\eta\rangle \in \mathbb{R}^m$, hence, $\langle \xi_i \rangle = 0$ and $\langle \xi_i \xi_j \rangle = \Gamma^{\text{II}}_{ij}$. Its m -th component takes the form of the generalized Langevin equation (GLE);

$$\sum_{j=1}^m \Gamma^{\text{II}}_{mj} \Delta z_j = f_m + \xi_m, \quad (10)$$

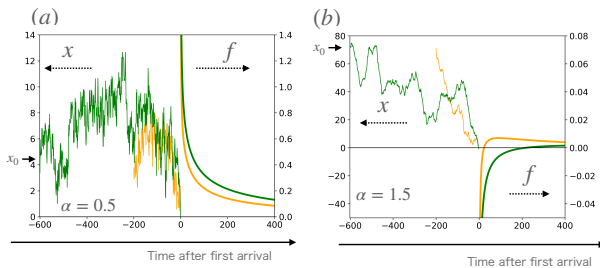


FIG. 2: Examples of first passage paths and resultant memory forces acting on the walker in subsequent process for (a) sub-diffusive fBm ($\alpha = 0.5$) and (b) superdiffusive fBm ($\alpha = 1.5$). The time axis is shifted to set the moment of the first passage to be origin.

which represents the force balance equation at time $N = n+m$ given the past history $\{x_i\}_0^{N-1}$. One can repeat the above argument by replacing m with $m' = N' - n$ ($< m$) along with the corresponding redefinitions of all the matrices and vectors ($\Gamma^{\text{II}} \in \mathbb{R}^{m' \times m'}$, $\Omega^{\text{T}} \in \mathbb{R}^{m' \times n}$, $|f\rangle \in \mathbb{R}^{m'}$ etc.), whereby construct the force balance equation at time $N' = n + m'$. Following the stochastic energetic definition of the heat [21], the quantity $\Delta' Q_{m'} := (-\sum_{j=1}^{m'} \Gamma^{\text{II}}_{m'j} \Delta z_j + \xi_{m'}) \Delta z_{m'} = -f_{m'} \Delta z_{m'}$ is interpreted as the absorbed heat in the step $x_{N'-1}$ to $x_{N'}$. Therefore, we identify $\Lambda[\{\Delta y_i\}, \{\Delta z_i\}] = -\langle \Delta z | f \rangle = \sum_{m'=1}^m \Delta' Q_{m'}$ as the total heat transfer to the system in the post first passage path $\{x_i\}_n^N$.

Noting $\Lambda[\{x_i\}_{0,n}^N] = -\Lambda[\{\bar{x}_i\}_{0,n}^N]$ in Eq. (5), one then pursues a standard line of argument by performing integral over dead paths with no restriction on the end-point $x_N \in (-\infty, \infty)$ to obtain

$$\frac{P_D(\Lambda, N|x_0)}{P_{\bar{D}}(-\Lambda, N|\bar{x}_0)} = \exp(-2\Lambda), \quad (11)$$

where $P_D(\Lambda, N|x_0)$ is the distribution of Λ after N steps for an ensemble of realization of the original dead process, and $P_{\bar{D}}(\Lambda, N|x_0)$ is defined in a parallel fashion for its reflected process. It follows the integral fluctuation theorem for Λ ; $\langle e^{2\Lambda} \rangle_D = 1$ and the ensuing inequality $\langle \Lambda \rangle_D \leq 0$ is interpreted as the second law, where $\langle \dots \rangle_D$ is the average over the properly normalized $P_D(\Lambda, N|x_0)$ conditional on the dead paths.

Now we modify the step described above by specifying the end-point after N steps. Defining $P_D(x, \Lambda, N|x_0)$ be the joint PDF of x and Λ , where x is the position of dead walkers after N steps starting at x_0 , and analogously $P_{\bar{D}}(x, -\Lambda, N|\bar{x}_0)$ for the reflected walkers, we obtain (see SI)

$$\frac{P_D(x, \Lambda, N|x_0)}{P_{\bar{D}}(x, -\Lambda, N|\bar{x}_0)} = \exp(-2\Lambda). \quad (12)$$

Integrating Eq. (12) over Λ then finds

$$\frac{P_D(x, N|x_0)}{P_{\bar{D}}(x, N|\bar{x}_0)} = \langle \exp(2\Lambda) \rangle_{\bar{D},x} = \langle \exp(2\Lambda) \rangle_{D,x}^{-1}, \quad (13)$$

where $\langle \dots \rangle_{D,x}$ stands for averaging over $P_D(\Lambda, N|x, x_0) = P_D(x, \Lambda, N|x_0)/P_D(x, N|x_0)$, and $\langle \dots \rangle_{\bar{D},x}$ is understood analogously. Imposing then the end-point to be in the physical domain ($x \geq 0$), use of Eq. (13) with Eq. (6) allows us to quantify the departure from the MI result in non-Markovian processes in terms of heat. In a similar way, one can obtain the expression of the survival probability in terms of the exponential average of the heat (see SI).

Discussions - Compared to Markovian systems, the behaviors of non-Markovian systems are more involved in many respects. A distinct feature of the latter can be seen in their conditional behaviors based on past history. With such information encoded, the PDF $P_D(x, N|x_0)$ of the dead walkers is non-trivial and difficult to specifically

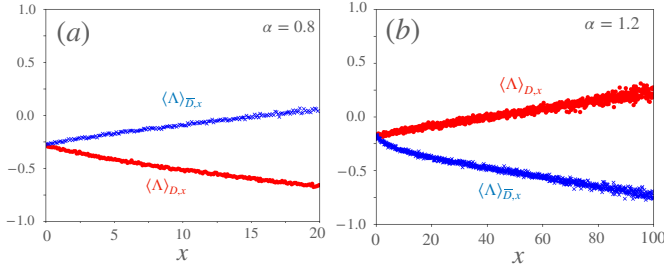


FIG. 3: Average heat flow in the post first passage process. (a) fBm with $\alpha = 0.8$ and (b) fBm with $\alpha = 1.2$. The starting position is $x_0 = 300^{\alpha/2}$. Average absorbed heat $\langle \Lambda \rangle_{D,x}$ along the dead paths (red) and $\langle \Lambda \rangle_{\overline{D},x}$ along the reflected paths (blue) are shown as functions of the end point $x (\geq 0)$ after $N = 10^3$ steps. Note that the relation $\langle \Lambda \rangle_{D,0} = \langle \Lambda \rangle_{\overline{D},0}$ holds due to symmetry.

express, whereas the unconditional PDF $P_0(x, N|x_0)$ is not. Indeed, the energetics of the unconditional non-Markovian process in absence of the potential landscape is as trivial as the corresponding Markovian process, i.e., in both cases, the viscous (or viscoelastic) resistance force and the noise balance to zero in overdamped limit, hence, no net energy flow between the system and the environment. For conditional non-Markovian processes, however, we have just seen that the process is biased due to the memory, putting the resulting energetics due to such a biasing force on the stage. Here, the relevant quantity is Λ , the heat flow to the system in the post first passage process.

Let us examine the statistical property of Λ . Figure 3 plots the average heat in the post first passage process as a function of its end point $x = x_N$ for subdiffusive and superdiffusive fBMs. Recall that $\langle \Lambda \rangle_{D,x}$ is the average heat absorption associated to dead paths conditioned on their initial ($x_0 > 0$) and final ($x_N \geq 0$) positions. At the same time, also of interest is the corresponding quantity $\langle \Lambda \rangle_{\overline{D},x}$ for the reflected paths, hence, conditioned on their initial ($\bar{x}_0 < 0$) and final ($x_N \geq 0$) positions. Applying Jensen's inequality to Eq. (13) provides bounds on the violation of the MI result;

$$\langle \Lambda \rangle_{\overline{D},x} \leq \frac{1}{2} \ln \left(\frac{P_D(x, N|x_0)}{P_0(x, N|-x_0)} \right) \leq -\langle \Lambda \rangle_{D,x}. \quad (14)$$

We quite generally observe that the heat emission on average into the environment $-\langle \Lambda \rangle_{D,x} > 0$. It is particularly true for anti-persistent process as might be naturally expected from $P_D(x, N|x_0) \geq P_0(x, N|-x_0)$ (Fig. 1(b)). Such a naive intuition, however, does not apply straightforwardly to persistent process, for which $P_D(x, N|x_0) \leq P_0(x, N|-x_0)$ (Fig. 1(c)). In addition, while the amount of heat emission increases with x for $\alpha < 1$, it decreases with x for $\alpha > 1$ and reverse sign for large x , i.e., starting from $\bar{x}_0 < 0$, reaching far in the positive domain requires heat absorption. We note that

it is compatible with the inequality (14), which ensures the positivity for the sum $-(\langle \Lambda \rangle_{D,x} + \langle \Lambda \rangle_{\overline{D},x})$ but not for individual terms.

The above results can be summarized into the following picture. During the initial first passage process $\{x_i\}_0^n$, the system interacts with the environment and builds correlation with it, creating a potential $U(x, t; |\Delta y\rangle) = -f(t; |\Delta y\rangle)x$ for the post first passage process $\{x_i\}_n^N$. Indeed, as observed in a tagged-monomer system projected from a polymer chain [32–37], non-Markovian processes usually imply the presence of hidden degrees of freedom, whose dynamics are slow enough in comparison to the system. The system exchanges energy with such a slowly fluctuating environment in the form of either heat or work. Taking the continuum form, the energy balance during the stochastic time evolution over time period dt [21] is written as

$$dU_t = -f dx_t - (\partial_t f) x_t dt, \quad (15)$$

where our definition of absorbed heat $d'Q_t = -f dx_t$ indicates $d'W_t := -(\partial_t f) x_t dt$ to be identified as the work done to the system.

In anti-persistent process, f is positive, thus, upon the first passage to $x = 0$, the walker tends to be pushed back into positive domain as reflected in $P_D(x, N|x_0) > P_0(x, N|-x_0)$ (Fig. 1(b)). Since the push-back motion corresponds to sliding down the potential, it accompanies the heat emission, but the temporally decaying nature of the force f indicates lifting up the potential (Eq. (15)) in positive domain, hence the work done to the system. This explains the observation $\langle \Lambda \rangle_{D,x=0} < 0$ even without net change in the potential value for such paths $x_n = 0 \rightarrow x_N = 0$ (see SI).

In contrast, f is initially negative in persistent process, whose magnitude decays with time (Fig. 2(b)). One might expect that the walker needs to absorb heat in climbing the potential to enter the positive domain. However, the inspection reveals that the walker typically slides down the potential at first toward the negative domain, providing an opportunity for the work due to potential lift to be done. Given this work, the walker needs to absorb less heat to later reach the positive domain such that the net heat absorption can be negative. In addition, f becomes positive in later time in typical cases (Fig. 2), though its magnitude is small, which also contributes to the trend. Still, the walker needs to absorb heat to reach far into the positive domain as exemplified in Fig. 3. These observations indicate the importance of relatively minor paths accompanying large heat absorption, which dominate the exponential average $\langle \exp(2\Lambda) \rangle_{D,x} > 0$ for $x > 0$ in Eq. (13), hence establish the spatial profile $P_D(x, t|x_0)$ of the dead walkers, see Fig. 1 (c).

Besides the path probability argument made so far, another view to arrive at the memory force “ f ” is a conversion from frictions to noises due to the temporal-origin shift in GLE, e.g., as, in continuous form, $\int_0^t ds \Gamma(t-s) \dot{x}_s = \xi_t \rightarrow \int_\tau^t ds \Gamma(t-s) \dot{x}_s = \xi'_t$ with mean zero

$\langle \xi_t \rangle = 0$, the variance $\langle \xi_t \xi_s \rangle = \Gamma(t - s)$, and the path-encoded noise $\xi'_t := \xi_t - \int_0^t ds \Gamma(t - s) \dot{x}_s$ with $0 < \tau < t$. The noise difference accounts for the heat identified by $\Lambda = \int_\tau^t dt' (\xi_{t'} - \xi'_{t'}) \dot{x}_{t'}$.

Finally, the fact that the heat Λ is related to the path correlation manifests in the relation $i_D[\{x_i\}_{0,n}^N] - i_{\bar{D}}[\{\bar{x}_i\}_{0,n}^N] = 2\Lambda[\{x_i\}_{0,n}^N]$ where $i_D[\{x_i\}_{0,n}^N] := \ln(P[\{x_i\}_{0,n}^N]/P[\{x_i\}_0^n]P[\{x_i\}_n^N])$ is the mutual information between pre- and post-first passage paths in a dead path, and $i_{\bar{D}}[\{\bar{x}_i\}_{0,n}^N]$ is defined similarly for the reflected path.

In summary, we have shown that the MI fails in non-Markovian processes due to the lack of reflection symmetry. The symmetry is broken by the memory effect, and its degree of the asymmetry manifests in the history dependent conditional probability, which is quantified by

the heat in the associated process. The statistics of the heat mirrors characteristic features of the process. It may be interesting to investigate the problem using, e.g., the Rouse polymer model [38], where the interaction between the system (in the present context, a tagged monomer in the polymer) and the environment (the rest of the polymer) can be explicitly analyzed [32–37]. We expect that elucidating the thermodynamic aspect of such a system may provide valuable insights into the first passage problem in non-Markovian processes.

Acknowledgement

This work was supported by JSPS KAKENHI (Grant No.JP23H00369 and JP24K00602).

-
- [1] J.D. Jackson, *Classical Electrodynamics, Third edition* (John Wiley & Sons, Inc.).
 - [2] W. Thomson, *Geometrical Investigations Regarding Spherical Conductors*, MacMillan & Co., (1849).
 - [3] J.R. Blake, Proc. Camb. Phil. Soc. **70**, 303 (1971).
 - [4] S. Redner, *A Guide to First-Passage Processes, First edition* (Cambridge University Press).
 - [5] S. Chandrasekhar, Rev. Mod. Phys. **15**, 1 (1943).
 - [6] A.V. Chechkin, V.Y. Gonchar, J. Klafter and R. Metzler, Adv. Chem. Phys. **133**, 439 (2006).
 - [7] Y. Kantor and M. Kardar, Phys. Rev. E **76**, 061121 (2007).
 - [8] A. Zoia, A. Rosso and M. Kardar, Phys. Rev. E **76**, 021116 (2007).
 - [9] R. Forsling, L. P. Sanders, T. Ambjörnsson, and L. Lizana, J. Chem. Phys. **141**, 094902 (2014).
 - [10] J.-H. Jeon, A. V. Chechkin, and R. Metzler, Europhys. Lett. **94**, 20008 (2011).
 - [11] A. Amitai, Y. Kantor and M. Kardar, Phys. Rev. E **81**, 011107 (2010).
 - [12] L.P. Sanders and T. Ambjörnsson, J. Chem. Phys. **7**, 175103 (2012).
 - [13] Y. Sakamoto and T. Sakaue, Phys. Rev. Res. **5**, 043148 (2023).
 - [14] C. Maes, SciPost Phys. Lect. Notes **32** (2021).
 - [15] U. Seifert, Rep. Prog. Phys. **75**, 126001 (2012).
 - [16] C. Jarzynski, Phys. Rev. X **7**, 011008 (2017).
 - [17] G.E. Crooks, Phys. Rev. E **61**, 2361 (2000).
 - [18] V.Y. Chernyak, M. Chertkov and C. Jarzynski, J. Stat. Mech. Theory Exp. **2006**, P08001 (2006).
 - [19] R. García-García, V. Lecomte, A.B. Kolton and D. Domínguez, J. Stat. Mech., **2012**, P02009 (2012).
 - [20] É. Roldán, I. Neri, R. Chetrite, S. Gupta, S. Pigolotti, F. Jülicher and K. Sekimoto, Adv. Phys. **72**, 1 (2023).
 - [21] K. Sekimoto, *Stochastic Energetics* (Springer-Verlag).
 - [22] J. R. M. Hosking, Water Resour. Res. **20**, 1898 (1984).
 - [23] T. Dieker, *Simulation of fractional Brownian motion*, PhD Thesis (Department of Mathematical Science, University of Twente, 2004).
 - [24] I.M. Sokolov, Soft Matter. **8**, 9043 (2012).
 - [25] R. Metzler, J.-H. Jeon, A.G. Cherstvy and E. Barkai, Phys. Chem. Chem. Phys., **16**, 24128 (2014).
 - [26] N.G. van Kampen, *Stochastic Processes in Physics and Chemistry, Third edition* (Elsevier, Amsterdam, 2007).
 - [27] G.W. Gardiner, *Handbook of Stochastic Methods for physics, chemistry and the Natural Sciences, Third edition* (Springer-Verlag, Berlin, 2004).
 - [28] J.-P. Bouchaud and A. Georges, Phys. Rep., **195**, 127-293 (1990).
 - [29] R. Kubo, M. Toda and N. Hashitsume, *Statistical Physics II. Nonequilibrium Statistical Mechanics* (Springer-Verlag).
 - [30] L. Onsager and S. Machlup, Phys. Rev. **91** 1505-1512 (1953).
 - [31] T. Ohkuma, and T. Ohta, J. Stat. Mech. **2007**, P10010 (2007).
 - [32] D. Panja, J. Stat. Mech. P06011 (2010).
 - [33] T. Sakaue, Phys. Rev. E **87**, 040601(R) (2013).
 - [34] C. Maes and S.R. Thomas, Phys. Rev. E **87**, 022145 (2013).
 - [35] T. Saito and T. Sakaue, Phys. Rev. E **92**, 012601 (2015).
 - [36] H. Vandeboek and C. Vanderzande, J. Stat. Phys. **167**, 14 (2017).
 - [37] T. Saito, Phys. Rev. E **105**, 014501 (2022).
 - [38] M. Doi and S.F. Edwards, *The Theory of Polymer Dynamics* (Clarendon, Oxford, UK, 1986).

Supplemental Information

This supplemental information is organized as follows. In Sec. I, we present a derivation of fluctuation theorem for Λ , which is Eq. (12) in the main text. Section II discusses an equality for the surviving probability, which is obtained by integrating Eq. (12) over Λ and $x (\geq 0)$. Finally, Sec. III describes a brief summary of numerical simulation method and some of supplemental numerical results related to the discussion in the main text.

I. FLUCTUATION THEOREM FOR Λ

We present a derivation of Eq. (12) in the main text. The probability $P_D(x, \Lambda, N|x_0)$ is obtained by extracting the paths with $\Lambda(\{\Delta x_i\}_{0,n}^N) = \Lambda$ and $x_N = x$ through an insertion of Dirac's delta into path integral of Eq. (2) in the main text. Using the path probability ratio (5) in the main text and the parity of $\Lambda(\{\Delta x_i\}_{0,n}^N)$, we proceed as

$$\begin{aligned} P_D(x, \Lambda, N|x_0) &= \sum_{n=1}^N \int D[\{x_i\}_{0,n}^N] P[\{x_i\}_{0,n}^N] \delta(x - x_N) \delta(\Lambda - \Lambda(\{\Delta x_i\}_{0,n}^N)) \\ &= \sum_{n=1}^N \int D[\{\bar{x}_i\}_{0,n}^N] P[\{\bar{x}_i\}_{0,n}^N] \exp[2\Lambda(\{\Delta \bar{x}_i\}_{0,n}^N)] \delta(x - x_N) \delta(\Lambda + \Lambda(\{\Delta \bar{x}_i\}_{0,n}^N)) \\ &= \exp(-2\Lambda) P_{\bar{D}}(x, -\Lambda, N|\bar{x}_0), \end{aligned} \quad (1)$$

where $\int D[\{x_i\}_{0,n}^N] := [\prod_{i=1}^n \int_0^\infty dx_i] [\prod_{i=n+1}^N \int_{-\infty}^\infty dx_i]$, $\int D[\{\bar{x}_i\}_{0,n}^N] := [\prod_{i=1}^n \int_{-\infty}^0 d\bar{x}_i] [\prod_{i=n+1}^N \int_{-\infty}^\infty d\bar{x}_i]$.

In Fig. 4, we show a numerical demonstration of the above relation. The collapse of $P_{\bar{D}}(x, -\Lambda, N|\bar{x}_0)e^{-2\Lambda}$ onto $P_D(x, \Lambda, N|x_0)$ (except for the skirt due to deteriorating sampling efficiency) supports Eq. (1).

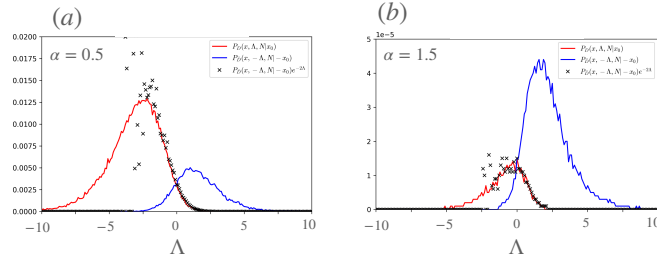


FIG. 4: Numerical plots of the key factors appearing in Eq. (1) for (a) subdiffusive fBm ($\alpha = 0.5$, $x = 5$, $x_0 = \sqrt{300\alpha}$, $N = 1 \times 10^3$) and (b) superdiffusive fBm ($\alpha = 1.5$, $x = 100$, $x_0 = \sqrt{300\alpha}$, $N = 1 \times 10^3$). Red or blue solid line represents $P_D(x, \Lambda, N|x_0)$ or, $P_{\bar{D}}(x, -\Lambda, N|\bar{x}_0)$, respectively. Black cross symbols indicate $P_{\bar{D}}(x, -\Lambda, N|\bar{x}_0)e^{-2\Lambda}$.

II. SURVIVAL PROBABILITY

One can also obtain the following expression for the survival probability $P_S(t, x_0) := \int_0^\infty dx P(x, t|x_0)$ by integration over the physical domain $x \geq 0$;

$$P_S(t, x_0) = \frac{1 + \text{erf}(x_0/\sigma_t)}{2} - \frac{1 - \text{erf}(x_0/\sigma_t)}{2\langle \exp(2\Lambda) \rangle_{D,+}}, \quad (2)$$

where $\sigma_t := [\int_{-\infty}^\infty dx (x - x_0)^2 P_0(x, t|x_0)]^{1/2}$ is the root mean-square displacement of the unrestricted walkers and $\langle \cdots \rangle_{D,+}$ denotes averaging over the distribution $\int_0^\infty dx P_D(x, \Lambda, t|x_0) / [\int_0^\infty dx P_D(x, t|x_0)]$.

Before deriving Eq. (2), we define the following quantities through integral of the probability distribution of the dead walkers $P_D(x, t|x_0)$;

$$\begin{aligned} H_D^+(t, x_0) &= \int_0^\infty dx P_D(x, t|x_0), \\ H_D^-(t, x_0) &= \int_{-\infty}^0 dx P_D(x, t|x_0), \end{aligned} \quad (3)$$

where the superscript $+$ or $-$ indicates the integral domain. Similarly, we define $H_D^+(t, \bar{x}_0)$, $H_D^-(t, \bar{x}_0)$ from $P_D(x, t|\bar{x}_0)$ and $H_0^+(t, x_0)$, $H_0^-(t, x_0)$ from $P_0(x, t|x_0)$. One can verify the following relations:

$$H_D^+(t, \bar{x}_0) = H_0^+(t, -x_0) = H_0^-(t, x_0), \quad (4)$$

where the first equality follows from Eq. (6) in the main text and the second equality is readily obtained by the change of the integration variable $x \rightarrow -x$.

To derive Eq. (2), we start from the relation $P_D(x, N|x_0) = P_{\bar{D}}(x, N|\bar{x}_0)\langle \exp(2\Lambda) \rangle_{\bar{D},x}$ or $P_D(x, N|x_0)\langle \exp(2\Lambda) \rangle_{D,x} = P_{\bar{D}}(x, N|\bar{x}_0)$ from Eq. (13) in the main text. Integrating the both sides of the equations over the physical domain $x \geq 0$, we find

$$\frac{H_D^+(N, x_0)}{H_D^+(N, x_0)} = \langle \exp(2\Lambda) \rangle_{\bar{D},+} = \langle \exp(2\Lambda) \rangle_{D,+}^{-1}, \quad (5)$$

where $\langle \cdots \rangle_{D,+}$ denotes averaging over $\int_0^\infty dx P_D(x, \Lambda, N|x_0)/[\int_0^\infty dx P_D(x, N|x_0)]$. Using Eqs. (4) and (5) and the definition of the survival probability $P_S(t, x_0) := \int_0^\infty dx P(x, t|x_0) = H_0^+(t, x_0) - H_D^+(t, x_0)$, we find

$$\begin{aligned} P_S(t, x_0) &= H_0^+(t, x_0) - \langle \exp(2\Lambda) \rangle_{\bar{D},+} H_0^-(t, x_0) \\ &= H_0^+(t, x_0) - H_0^-(t, x_0)/\langle \exp(2\Lambda) \rangle_{D,+}. \end{aligned} \quad (6)$$

For Gaussian processes, the distribution of unrestricted walkers starting from $x = x_0$ is

$$P_0(x, t|x_0) = \frac{1}{\sqrt{2\pi\sigma_t^2}} \exp\left(-\frac{(x-x_0)^2}{2\sigma_t^2}\right) \quad (7)$$

and its integral over physical (positive) or negative domain is represented with the error function $\text{erf}(x) := (2/\sqrt{\pi}) \int_0^x e^{-y^2} dy$;

$$H_0^\pm(t, x_0) = \frac{1}{2} \left(1 \pm \text{erf}\left(\frac{x_0}{\sigma_t}\right) \right) \quad (8)$$

with the double sign in the same order. Combining Eqs. (6) and (8), we obtain Eq. (2).

III. NUMERICAL SIMULATIONS

This section notes the numerical scheme throughout the article and supplemental data. The one-dimensional motion set off from x_0 is updated by iterating

$$\frac{x_i - x_{i-1}}{\Delta t} = \zeta_i, \quad (9)$$

where i denotes the number of the steps in the recursive loop with Δt being a step size, and ζ_i denotes the noises. The limit $\Delta t \rightarrow +0$ reduces eq. (9) into the equation of motion $dx_t/dt = \zeta_t$ at a time $t (= i\Delta t)$ in the continuum picture. Unless otherwise stated, the numerical simulations consider dimensionless unit and set $\Delta t = 1$.

The statistics of the noises $\{\zeta_i\}_0^N$ dictates the stochastic processes. Colored noises of the nonMarkovian fBms are generated according to the Hosking method [22, 23]. For Markovian walkers ($\alpha = 1$), $\{\zeta_i\}_0^N$ is simply taken from independently and identically distributed Gaussian noise.

A. Supplemental figures

a. Conditional path From an ensemble of paths starting from $x = x_0$, we extract paths, which arrive at $x = 0$ for the first time at $i = n$, and visit $x = x^*$ at $i = N$. Here we call such paths *conditional paths*. Note that the last condition does not require the first visit, i.e., after $i = n$, the multiple visits to $x = x^*$ are allowed. In Fig. 5, we show sample averages of such conditional paths with $x^* = 0$ for (a) sub-diffusive and (b) super-diffusive fBMs. Although plotted paths look quite irregular due to the limited number of sample paths, one can conceive a clear tendency that (a) sub-diffusive conditional paths are pulled back to the physical domain $x > 0$ after touching $x = 0$, (b) super-diffusive conditional paths are prone to keep the moving direction.

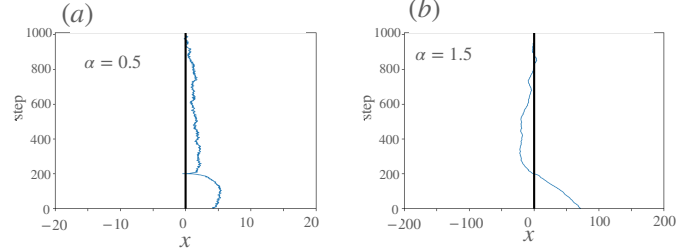


FIG. 5: Sample averages of conditional paths with $x^* = 0$ for (a) subdiffusive fBm ($\alpha = 0.5$) with $x_0 = \sqrt{300^\alpha}$, $n = 200$, $N = 1 \times 10^3$ and (b) superdiffusive fBm ($\alpha = 1.5$) with $x_0 = \sqrt{300^\alpha}$, $n = 200$, $N = 1 \times 10^3$. The averaging is done with 71 sample paths for (a) and 30 sample paths for (b).

b. Average heat flow in the post first passage process Average heat flow in the post first passage process is plotted in the Fig. 3 in the main text for the case of subdiffusive fBm $\alpha = 0.8$ and superdiffusive fBm $\alpha = 1.2$ cases. Here, we plot the same quantity for the cases of $\alpha = 0.5$ and $\alpha = 1.5$.

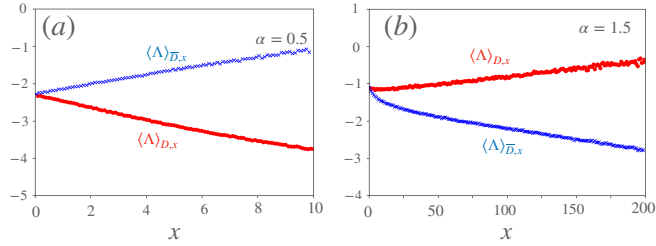


FIG. 6: Average heat flow in the post first passage process. (a) fBm with $\alpha = 0.5$ and (b) fBm with $\alpha = 1.5$. The starting position is $x_0 = 300^{\alpha/2}$. Average absorbed heat $\langle \Lambda \rangle_{D,x}$ along the dead paths (red) and $\langle \Lambda \rangle_{\bar{D},x}$ along the reflected paths (blue) are shown as functions of the end point $x (\geq 0)$ after $N = 10^3$ steps. Note that the distribution of these heats are shown in Fig. 4.